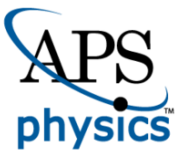

Interacting Surface States of Three-Dimensional Topological Insulators

Titus Neupert, Stephan Rachel, Ronny Thomale, and Martin Greiter

Phys. Rev. Lett. **115**, 017001 — Published 29 June 2015

DOI: 10.1103/PhysRevLett.115.017001

Interacting surface states of three-dimensional topological insulators

Titus Neupert,[1] Stephan Rachel,[2] Ronny Thomale,[3] and Martin Greiter[3]

[1] *Princeton Center for Theoretical Science, Princeton University, Princeton, New Jersey 08544, USA*
[2] *Institute for Theoretical Physics, Technische Universitaet Dresden, 01171 Dresden, Germany*
[3] *Institute for Theoretical Physics, University of Würzburg, Am Hubland, D-97074 Würzburg, Germany*

(Dated: June 1, 2015)

We numerically investigate the surface states of a strong topological insulator in the presence of strong electron-electron interactions. We choose a spherical topological insulator geometry to make the surface amenable to a finite size analysis. The single-particle problem maps to that of Landau orbitals on the sphere with a magnetic monopole at the center that has unit strength and opposite sign for electrons with opposite spin. Assuming density-density contact interactions, we find superconducting and anomalous (quantum) Hall phases for attractive and repulsive interactions, respectively, as well as chiral fermion and chiral Majorana fermion boundary modes between different phases. Our setup is preeminently adapted to the search for topologically ordered surface terminations that could be microscopically stabilized by tailored surface interaction profiles.

Introduction.—Three-dimensional topological insulators (3DTIs) [1–6] were predicted in 2007 and have been discovered subsequently in various material classes [7–11]. When viewed as a symmetry-protected topological phase [12], 3DTIs exhibit a gapped bulk with two-dimensional gapless edge states protected by U(1) electron number conservation and time reversal symmetry (TRS), forbidding any adiabatic deformation into a trivial insulator.

When the protecting U(1) particle number symmetry is broken, such as by a superconducting proximity effect, the 3DTI surface yields an unconventional gapped s-wave superconductor with Majorana modes in its vortex cores [13]. Upon breaking TRS, such as by a magnetic coating on the surface, the single surface Dirac cone gaps out, and the Chern-Simons boundary term of the axion bulk action manifests itself as a $\nu = 1/2$ quantum Hall effect [14] without fractionalized excitations. The axion term implies the Witten effect [15] by which an odd-half integer charge binds to magnetic monopoles in the bulk of a 3DTI (see also e.g. Ref. 16).

The aforementioned properties of 3DTIs do not involve interactions in the bulk or at the surface. Assuming that the gapped 3DTI bulk is negligibly renormalized by interactions, it remains to be investigated how interactions could affect the 3DTI surface. To begin with, interactions could contribute to breaking the protecting symmetries explicitly or spontaneously. Transcending the mean-field picture, however, interactions could also give rise to a gapped surface state with intrinsic topological order, allowing a new kind of phase to enter the realm of competing quantum states of matter on a 3DTI surface. Investigations of bosonic 3DTI surface states established that such gapped surface states in the absence of symmetry breaking are indeed possible for certain kinds of topological order [16–20]. Soon thereafter, this idea has been formulated for the physically more relevant fermionic analogue [21–24]. All these conceptually important works rely on consistency arguments on the level of topological field theories and constructions that employ contrived exactly soluble models. What type of physically attainable Hamiltonians would exhibit these exotic ground states remains a challenging question. [25]

From the viewpoint of Fermiology, the impact of interactions on 3DTI surface states appears related to the problem of interacting Dirac metals at charge neutrality in two spatial dimensions such as graphene. (For an early study, see e.g. Ref. [26].) With four Dirac cones in graphene formed by spin and valley degrees of freedom as opposed to one on 3DTI surfaces, however, several instabilities for the former do not apply to the latter. For instance, antiferromagnetism would be driven by intercone scattering centered at different momenta, while an exciton insulator [27] might not be excluded a priori.

Haldane [28] has recently pointed out that, as the topological surface state only has support in a 2D k-space region with an area A_k that may be much smaller that the Brillouin zone, the surface electrons obey an "uncertainty principle" where they cannot be localized within an area smaller than $(2\pi)^2/A_k$, analogous to the "magnetic area" $h/|eB|$ for electrons confined to a 2D Landau level. Ref. [28] noted that this makes the surface dynamics insensitive to the atomic-scale features of the surface, rendering exact diagonalization (ED) studies of such strongly-interacting systems practicable.

In this Letter, we develop a microscopic set-up for numerical studies of interactions on 3DTI surfaces. We employ a spherical geometry [29] and numerically investigate the phase diagram for both attractive and repulsive density-density contact interaction U. We find a superconducting phase for attractions, and ferromagnetic phases of broken TRS for repulsions. These are the $\nu = 1/2$ anomalous quantum Hall effect and the gapless anomalous Hall effect for fillings at and away from the Dirac point, respectively.

3DTI surface states on the sphere.—In the limit of long wavelengths, the surface states of a strong 3DTI are de-

scribed by a two-dimensional Dirac equation given by

$$H = v\hat{\boldsymbol{n}}\,(-\mathrm{i}\nabla\times\boldsymbol{\sigma}) \tag{1}$$

where v denotes the Dirac velocity of the surface states, $\hat{\boldsymbol{n}}$ is the surface normal, and $\boldsymbol{\sigma}=(\sigma_\mathrm{x},\sigma_\mathrm{y},\sigma_\mathrm{z})$ twice the physical electron spin vector. For a spherical TI with radius R, Imura et al. [29] derived that (1) becomes

$$H_0 = \frac{v}{R}\,(\sigma_\mathrm{x}\Lambda_\theta + \sigma_\mathrm{y}\Lambda_\varphi) \tag{2}$$

where

$$\boldsymbol{\Lambda} \;=\; -i\left[\boldsymbol{e}_\varphi\frac{\partial}{\partial\theta} - \boldsymbol{e}_\theta\frac{1}{\sin\theta}\left(\frac{\partial}{\partial\varphi} - \frac{\mathrm{i}}{2}\sigma_\mathrm{z}\cos\theta\right)\right] \tag{3}$$

is the dynamical angular momentum of an electron in the presence of a magnetic monopole with strength $2\pi\sigma_\mathrm{z}$, and (r,θ,φ) are spherical coordinates. The monopole strength or Berry flux through the sphere is hence 2π for $\uparrow$ spins (i.e., spins pointing in $\boldsymbol{e}_\mathrm{r}$ direction) and -2π for $\downarrow$ spins (i.e., spins pointing in $-\boldsymbol{e}_\mathrm{r}$ direction) [32]. The origin of this Berry phase is easily understood. Since the coordinate system for our spins (to which our Pauli matrices $\sigma_\mathrm{x},\sigma_\mathrm{y},\sigma_\mathrm{z}$ refer to) is given by $\boldsymbol{e}_\varphi,-\boldsymbol{e}_\theta,\boldsymbol{e}_\mathrm{r}$, it will rotate as the electron is taken around the sphere. For general trajectories, the Berry phase generated by this rotation is given by $\frac{1}{2}$ times the solid angle subtended by the trajectory. Formally, this phase is generated by a monopole with strength 2π at the origin. Since the model preserves time reversal invariance, the monopole must be of opposite sign for opposite spins.

Substitution of (3) into (2) yields $H_0=\frac{v}{R}\,h_0$ with

$$h_0 = \begin{pmatrix} 0 & h^+ \\ h^- & 0\end{pmatrix},\quad h^\pm = \mp\left(\partial_\theta + \frac{1}{2}\cot\theta\right) + \frac{\mathrm{i}\partial_\varphi}{\sin\theta}. \tag{4}$$

Eq. (4) describes a Dirac Hamiltonian in the sense that

$$h_0^2 = \begin{pmatrix} h^+h^- & 0 \\ 0 & h^-h^+\end{pmatrix} = \begin{pmatrix} \boldsymbol{\Lambda}^2_{s_0=+\frac{1}{2}} & 0 \\ 0 & \boldsymbol{\Lambda}^2_{s_0=-\frac{1}{2}}\end{pmatrix} + \frac{1}{2} \tag{5}$$

is diagonal. Apart from an overall numerical factor,

$$\boldsymbol{\Lambda}^2_{s_0} = -\frac{1}{\sin\theta}\partial_\theta\,(\sin\theta\,\partial_\theta) - \frac{1}{\sin^2\theta}\,(\partial_\varphi - \mathrm{i}s_0\cos\theta)^2 \tag{6}$$

is the Hamiltonian of an electron moving on a sphere with a monopole of strength $4\pi s_0$ in the center [30, 31]. The Landau levels on the sphere are spanned by two mutually commuting SU(2) algebras, one for the cyclotron momentum ($\boldsymbol{S}$) and one for the guiding center momentum ($\boldsymbol{L}$). The Casimir of both is given by $\boldsymbol{L}^2=\boldsymbol{S}^2=s(s+1)$, where $s=|s_0|+n$ and $n=0,1,\ldots$ is the Landau level index. With $\boldsymbol{\Lambda}^2=\boldsymbol{L}^2-s_0^2=(n+1)^2-\frac{1}{2}$ for $|s_0|=\frac{1}{2}$, we see that the eigenvalues of h_0^2 are given by $\epsilon^2=(n+1)^2$.

In terms of the spinor coordinates $u=\cos\frac{\theta}{2}e^{i\frac{\varphi}{2}}$, $v=\sin\frac{\theta}{2}e^{-i\frac{\varphi}{2}}$ introduced by Haldane [30], and their complex conjugates $\bar{u}$, $\bar{v}$,

$$S^+ = u\partial_{\bar{v}} - v\partial_{\bar{u}},\quad S^- = \bar{v}\partial_u - \bar{u}\partial_v,$$

$$S^\mathrm{z} = \tfrac{1}{2}(u\partial_u + v\partial_v - \bar{u}\partial_{\bar{u}} - \bar{v}\partial_{\bar{v}}), \tag{7}$$

$$L^+ = u\partial_v - \bar{v}\partial_{\bar{u}},\quad L^- = v\partial_u - \bar{u}\partial_{\bar{v}},$$

$$L^\mathrm{z} = \tfrac{1}{2}(u\partial_u - v\partial_v - \bar{u}\partial_{\bar{u}} + \bar{v}\partial_{\bar{v}}). \tag{8}$$

The physical Hilbert space is restricted to states with S^z eigenvalue s_0, $S^\mathrm{z}\phi = s_0\phi$ [31]. With the $\uparrow$ and $\downarrow$ spin components of the eigenstates of h_0 thus restricted respectively (i.e., $S^\mathrm{z}\phi^\uparrow=\frac{1}{2}\phi^\uparrow$ and $S^\mathrm{z}\phi^\downarrow=-\frac{1}{2}\phi^\downarrow$), it is easy to show that $h^-\phi^\uparrow=-S^-\phi^\uparrow$ and $h^+\phi^\downarrow=-S^+\phi^\downarrow$, and hence that

$$h_0 = \begin{pmatrix} 0 & -S^+ \\ -S^- & 0\end{pmatrix}. \tag{9}$$

The Dirac property of h_0 and the eigenvalues of h_0^2 imply that the eigenstates take the form

$$h_0\psi^\lambda_{nm} = \lambda(n+1)\psi^\lambda_{nm},\quad \psi^\lambda_{nm} = \begin{pmatrix}\phi^\uparrow_{nm} \\ \lambda\phi^\downarrow_{nm}\end{pmatrix}, \tag{10}$$

where $\lambda=\pm1$ distinguishes positive and negativ energy solutions, and m is the eigenvalue of L^z. With $h^+h^-=S^-S^++1$, we find [31]

$$\phi^\uparrow_{nm} = (L^-)^{s-m}(S^-)^n u^{2s} = (L^-)^{s-m}\,\bar{v}^n u^{n+1}, \tag{11}$$

where $s=n+\frac{1}{2}$ and $m=-s,-s+1,\ldots,s$. With (10),

$$\phi^\downarrow_{nm} = -\frac{S^-}{n+1}\phi^\uparrow_{nm} = -(L^-)^{s-m}\,u^n\bar{v}^{n+1}. \tag{12}$$

The number of degenerate states in the $(n+1)$-th Landau level with energy $\epsilon=\lambda(n+1)$ is hence $2(n+1)$, and grows linearly with $|\epsilon|$, as required for a Dirac cone [see Fig. 1 a)].

H_0 is invariant under both time reversal $\mathrm{T}\equiv-\mathrm{i}\sigma_\mathrm{y}\mathrm{K}$ (where K denotes complex conjugation) and parity $\mathrm{P}\equiv\sigma_\mathrm{x}\mathrm{P}_\theta$ (where P_θ takes $\theta\to\pi-\theta$). The basis states (10) transform according to

$$\mathrm{T}\psi^\lambda_{nm} = \lambda\,(-1)^{m-\frac{1}{2}}\,\psi^\lambda_{n,-m}, \tag{13}$$

$$\mathrm{P}\psi^\lambda_{nm} = \lambda\,(-1)^{n+m+\frac{1}{2}}\,\psi^\lambda_{n,m}. \tag{14}$$

Momentum space cutoff.—The Dirac Hamiltonian H_0 (or h_0) governs the behavior of the surface states of a topological insulator for energies close to the Dirac nodal point. At higher and lower energies, the surface states merge with the bulk conduction and valence bands, respectively, and their weight on the surface diminishes. Consequently, even strong electron-electron interactions of the order of the bulk gap will only induce small matrix elements between bulk and surface states. It is hence sensible to study the effects of strong interactions on the surface states alone, when working in the Fock space constructed from the single-particle eigenstates of H_0 with $(1+n)v/R<\Lambda$, where Λ is a cut-off energy imposed by the bulk energy gap. Importantly, it is impossible

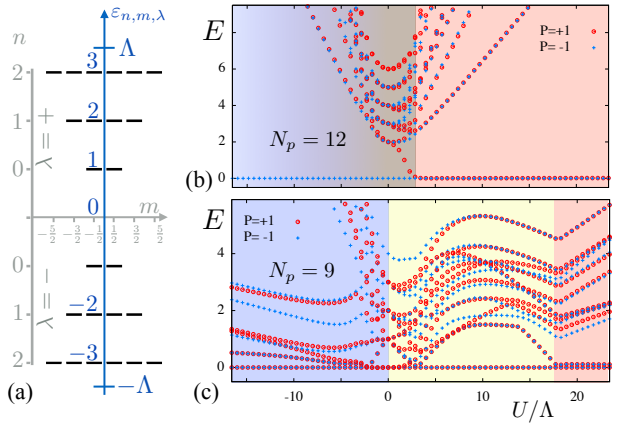

FIG. 1. (Color online) (a) Single-particle spectrum of the surface states of a spherical topological insulator topological for $n \leq 2$. (b) and (c) Exact diagonalization spectra for the topological insulator surface states subject to the contact interaction (15) for a Hilbert space restriction $n \leq 2$ as a function of interaction strength U/Λ for b) $N_p = 12$ and c) $N_p = 9$. We find s-wave superconductor (SC, blue) an anomalous Hall effect (AHE, red) coinciding with ferromagnetism that becomes a gapped anomalous quantum Hall phase (AQHE) at half filling. Two gapless phases include the semimetal (SM, green) at half filling and a Fermi liquid (FL, yellow). The FL is the region in phase space where we do not observe an ordered or gaped ground state. Together with the numerical results for the spin polarization, these spectra lead to the phase diagram Fig. 2.

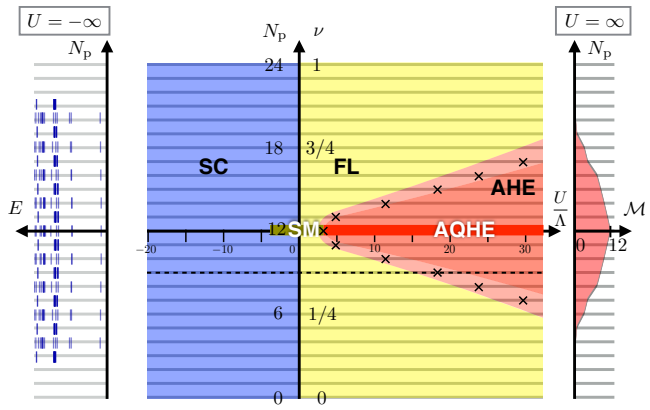

FIG. 2. (Color online) Phase diagram for the same model as in Fig. 1 as a function of interaction strength U/Λ and filling $\nu = N_p/[2(n_0+1)(n_0+2)]$, with the same color code for the phases. Left end of the energy spectrum in the limit $U/\Lambda \to -\infty$ as a function of the particle number N_p. The superconducting ground state is evidenced by the degeneracy of the ground states in all sectors of even N_p. Right panel: Magnetization $\mathcal{M}$ of the 2-fold (4-fold) quasi-degenerate ground state manifold in the limit $U/\Lambda \to \infty$ as a function of the even (odd) N_p. It evidences spontaneously broken TRS in the thermodynamic limit.

to build orbitals in position space that are localized on length scales smaller than $2\pi v/\Lambda$ in this restricted Hilbert space. Thus even if the interaction energy scales are much larger than Λ, the problem does not reduce to a classical limit [28]. This is somewhat reminiscent of the Landau level problem, with the important difference that single-particle states are exponentially localizable on long enough distances on the topological insulator surface while they are power-law decaying in a Landau level on a compact manifold.

Interactions.—On this restricted single particle Hilbert space, we consider a contact interaction

$$H_{\rm int} = U \int_{S_2} \mathrm{d}^2\, \boldsymbol{r} \rho_\downarrow(\boldsymbol{r}) \rho_\uparrow(\boldsymbol{r}), \qquad (15)$$

where $\rho_s(\boldsymbol{r})$ is the density operator of electrons with spin s at position $\boldsymbol{r}$. This interaction preserves T, P, the number of particles N_p, and the total angular momentum $M = \sum_{i=1}^{N_p} m_i$. We have studied the phase diagram of this model as a function of U/Λ and electron filling via exact diagonalization up to $n = 2$ ($\Lambda = 3.5v/R$, 24 single particle states) (see Fig. 2).

Magnetic phases.—At half filling and for $U/\Lambda > 3$, the ground state is a ferromagnet. In the finite system, we find two quasi-degenerate ground states $|\mathrm{FM}_\pm\rangle$ with $\mathrm{P} = \pm 1$ in the $M = 0$ sector. The magnetization operator in $\boldsymbol{e}_r$ direction, $\Sigma_3 \equiv \int_{S_2} \mathrm{d}^2\boldsymbol{r}\, [\rho_\uparrow(\boldsymbol{r}) - \rho_\downarrow(\boldsymbol{r})]$, anticommutes with the parity operator P, since $\Sigma_3\, \psi^\lambda_{nm} = \psi^{-\lambda}_{nm}$. This implies that $\langle \mathrm{FM}_+|\Sigma_3|\mathrm{FM}_+\rangle = \langle \mathrm{FM}_-|\Sigma_3|\mathrm{FM}_-\rangle = 0$. The magnetization of the ferromagnetic ground states with spontaneously broken TRS, which emerge in the thermodynamic limit, is hence given by $\mathcal{M} \equiv \langle \mathrm{FM}_+|\Sigma_3|\mathrm{FM}_-\rangle$. A ferromagnetically ordered gapped surface termination of a 3D topological insulator features a half-integer Hall effect—a phase that would not be possible in a pure 2D system without intrinsic topological order. Thus, the ferromagnetic phase also constitutes an anomalous quantum Hall phase. Between two domains of opposite magnetization, there exists a chiral boundary state (see Fig. 3a). Upon hole- or electron doping the anomalous quantum Hall phase, the system enters a anomalous Hall phase without a quantized Hall conductance. This phase can be distinguished from the anomalous quantum Hall phase by the scaling of its (finite size) gap with U: It converges to a constant for large U, while in the incompressible phase the gap does not saturate as U is increased. At high doping, the ground state is a Fermi liquid which does not violate any symmetry. We distinguish these two phases by the different quasi-degeneracies of the ground state and by computing the magnetization $\mathcal{M}$ in this quasi-degenerate subspace [see Fig. 1 b) and c)] [33].

While the small number of numerically amenable system sizes (possible values for the cutoff) does not allow for a proper extrapolation to the thermodynamic limit, a comparison of data for $n < 3$ not shown here indicates

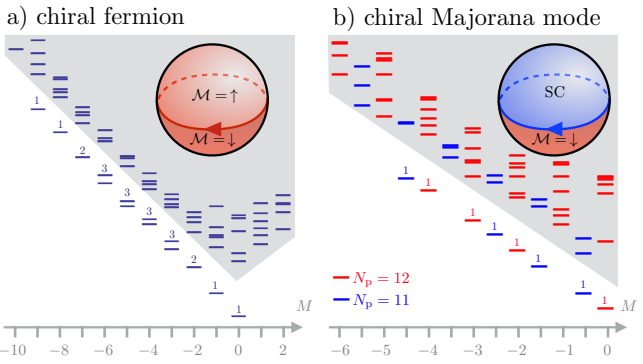

FIG. 3. (Color online) Numerical evidence for the emergence of (a) a chiral fermionic mode and (b) a chiral Majorana mode at the boundary between two ferromagnetic domains and a ferromagnet-superfluid domain wall, respectively. Shown are finite size energy spectra for a system restricted to the $n \leq 2$. Magnetic domains on the northern/southern hemisphere are enforced by Hamiltonian (2) with a mean-field magnetization $m_z(\theta)\sigma_z$ with $|m_z| = \Lambda$, while the superfluid domain is interaction-induced with $U = -4.3\Lambda$. In (a), the level counting is the one expected for a U(1) mode that consists of six states with $m = -5/2, \cdots, 5/2$ assuming that the levels with $m > 0$ are occupied in the half-filled ground state. In (b), the level counting in the fermion parity sectors are as expected if one assumes that the chiral Majorana mode at the boundary consists of three operators with $m = -5/2, -3/2, -1/2$ which do not annihilate the ground state.

that the onset of the ferromagnetic phase should remain at $U/\Lambda \sim 3$ in this limit. Unfortunately, our finite size studies cannot preclude the appearance of new phases in larger systems, a concern which may be of particular validity near the quantum critical point.

Superfluid phase.—At negative U, the system enters a superfluid phase. We see this from even-odd oscillations of the ground state energy as a function of particle number found in the entire range of negative U as well as a quadratically dispersing mode in the even N_p sectors noticeable for $U/\Lambda \lesssim -1$, that is the precursor of the superfluid's Goldstone mode in the thermodynamic limit. For $U/\Lambda \to -\infty$, this mode becomes exactly flat, i.e., we observe a set of degenerate states at $M = 0$, one in each sector of even N_p (see Fig. 2). The low energy excitations above the ground state in each sector of even N_p show the same structure as the spectrum of two electrons subject to an infinite repulsive interaction, which consists of three quasi-degenerate states with $M = -1, 0, 1$. This suggests that the low-energy excitations in the superfluid phase are obtained by breaking up an individual Cooper pair into two electrons which do not interact with the condensate. An s-wave superconducting termination of a 3D topological insulator is a topological superconductor in the sense that it supports Majorana zero energy states in vortex cores and a chiral Majorana mode at the boundary with e.g. a ferromagnetic region of the surface (see Fig. 3b). That we obtain a gapped superconducting state in the limit $U/\Lambda \to -\infty$ is a direct manifestation of the localization properties of the single-particle states. If the single particle states were fully localizable in real space, pairs of electrons could bind into point-like particles and the ground state would be exponentially degenerate.

Conclusions.—We have developed a formalism to study interaction effects on fermionic 3DTI surface states numerically. From the analysis of a two-body contact interaction, we found both ferromagnetic and topologically non-trivial superconducting phases, as well as chiral fermion and chiral Majorana fermion boundary modes between different phases. Several branches of future investigation can be anticipated, such as the application to bosons and studies of more sophisticated interaction profiles. The formalism establishes an ideal testing ground for topologically ordered TI surface state scenarios.

T.N. acknowledges several fruitful discussions with F.D.M. Haldane and thanks him for sharing the results of Ref. [28] prior to publication. R.T. thanks T. Dumitrescu and M. Metlitski for discussions. This work was supported by DARPA SPAWARSYSCEN Pacific N66001-11-1-4110, by the Helmholtz association through VI-521, by the DFG through FOR 960 and SPP 1666, and by the European Research Council through the grant TOPOLECTRICS (ERC-StG-Thomale-336012).

[1] R. Roy, Phys. Rev. B **79**, 195322 (2009).
[2] J. E. Moore and L. Balents, Phys. Rev. B **75**, 121306 (2007).
[3] L. Fu, C. L. Kane, and E. J. Mele, Phys. Rev. Lett. **98**, 106803 (2007).
[4] L. Fu and C. L. Kane, Phys. Rev. B **76**, 045302 (2007).
[5] M. Z. Hasan and C. L. Kane, Rev. Mod. Phys. **82**, 3045 (2010).
[6] X.-L. Qi and S.-C. Zhang, Rev. Mod. Phys. **83**, 1057 (2011).
[7] D. Hsieh, D. Qian, L. Wray, Y. Xia, Y. S. Hor, R. J. Cava, and M. Z. Hasan, Nature **452**, 970 (2008).
[8] D. Hsieh *et al.*, Science **323**, 919 (2009).
[9] Y. Xia *et al.*, Nature Physics **5**, 398 (2009).
[10] H. Zhang, C.-X. Liu, X.-L. Qi, X. Dai, Z. Fang, and S.-C. Zhang, Nature Physics **5**, 438 (2009).
[11] Y. L. Chen *et al.*, Science **325**, 178 (2009).
[12] C. Wang, A. C. Potter, and T. Senthil, Science **343**, 629 (2014).
[13] L. Fu and C. L. Kane, Phys. Rev. Lett. **100**, 096407 (2008).
[14] X.-L. Qi, T. L. Hughes, and S.-C. Zhang, Phys. Rev. B **78**, 195424 (2008).
[15] E. Witten, Phys. Lett. B **86**, 283 (1979).
[16] M. A. Metlitski, C. L. Kane, and M. P. A. Fisher, Phys. Rev. B **88**, 035131 (2013).
[17] A. Vishwanath and T. Senthil, Phys. Rev. X **3**, 011016 (2013).
[18] C. Wang and T. Senthil, Phys. Rev. B **87**, 235122 (2013).
[19] F. J. Burnell, X. Chen, L. Fidkowski, and A. Vishwanath, Phys. Rev. B **90**, 245122 (2014).

[20] S. Geraedts and O. Motrunich, arXiv:1408.1096.
[21] M. A. Metlitski, C. L. Kane, and M. P. A. Fisher, arXiv:1306.3286.
[22] C. Wang, A. C. Potter, and T. Senthil, Phys. Rev. B **88**, 115137 (2013).
[23] P. Bonderson, C. Nayak, and X.-L. Qi, J Stat Mech: Theo Exp **2013**, P09016 (2013).
[24] L. Fidkowski, X. Chen, and A. Vishwanath, Phys. Rev. X **3**, 041016 (2013).
[25] D. F. Mross, A. Essin, and J. Alicea, arXiv:1410.4201.
[26] J. González, F. Guinea, and M. A. H. Vozmediano, Phys. Rev. B **63**, 134421 (2001).
[27] D. T. Son, Phys. Rev. B **75**, 235423 (2007).
[28] F. D. M. Haldane, talk "'Quantum Geometry' and Topological Insulators" at Nobel symposium on "New forms of matter: topological insulators and superconductors", Stockholm, Sweden, 06/14/2014, and private communication.
[29] K.-I. Imura, Y. Yoshimura, Y. Takane, and T. Fukui, Phys. Rev. B **86**, 235119 (2012).
[30] F. D. M. Haldane, Phys. Rev. Lett. **51**, 605 (1983).
[31] M. Greiter, Phys. Rev. B **83**, 115129 (2011).
[32] Note that the sign of the monopole strength is reversed as compared to [29], since we use a notation where we couple to electrons with charge $-e$.
[33] Phases that become gapless in the thermodynamic limit are hard to detect and discriminate using numerially exact diagonalization. Thus, we expect that the location of all the phase transition points that we determine as a function of U are subject to strong finite-size errors. Since we understand the limits at $U = +\infty$, $U = 0$ and $U = -\infty$, however, the structure of the phase diagram is fixed.